Hydrophilic interaction liquid chromatography: An efficient tool for assessing thorium interaction with phosphorylated biomimetic peptides

Lana Abou-Zeid, Albert Pell, Marina Amaral Saraiva, Pascale Delangle, Carole Bresson

Journal of Chromatography A 1735 (2024) 465341

Contents lists available at ScienceDirect

Journal of Chromatography A

journal homepage: www.elsevier.com/locate/chroma

Hydrophilic interaction liquid chromatography: An efficient tool for assessing thorium interaction with phosphorylated biomimetic peptides

Lana Abou-Zeid [a,c,1], Albert Pell [a], Marina Amaral Saraiva [a], Pascale Delangle [b], Carole Bresson [a,*]

[a] Université Paris-Saclay, CEA, Service de Physico Chimie, Gif-sur-Yvette F-91191, France
[b] Université Grenoble Alpes, CEA, CNRS, Grenoble INP, IRIG, SyMMES, Grenoble 38 000, France
[c] Sorbonne Université, UPMC, Paris F-75005, France

ARTICLE INFO

Keywords:
Thorium
Phosphorylated peptides
Affinity
Competition
HILIC
ESI-MS
ICP-MS

ABSTRACT

In the field of nuclear toxicology, the knowledge of the interaction of actinides (An) with biomolecules is of prime concern in order to elucidate their toxicity mechanism and to further develop selective decorporating agents. In this work, we demonstrated the great potential of hydrophilic interaction liquid chromatography (HILIC) to separate polar thorium (Th) biomimetic peptide complexes, as a key starting point to tackle these challenges. Th^{4+} was used as plutonium (Pu^{4+}) analogue and pS16 and pS1368 as synthetic di- and tetra-phosphorylated peptides capable of mimicking the interaction sites of these An in osteopontin (OPN), a hyperphosphorylated protein. The objective was to determine the relative affinity of pS16 and pS1368 towards Th^{4+}, and to evaluate the pS1368 selectivity when Th^{4+} was in competition complexation reaction with UO_2^{2+} at physiological pH. To meet these aims, HILIC was simultaneously coupled to electrospray ionization mass spectrometry (ESI-MS) and inductively coupled plasma mass spectrometry (ICP-MS), which allowed to identify online the molecular structure of the separated complexes and quantify them, in a single step. Dedicated HILIC conditions were firstly set up to separate the new dimeric $Th_2(peptide)_2$ complexes with good separation resolution (peptide = pS16 or pS1368). By adding pS16 and pS1368 in different proportions relatively to Th^{4+}, we found that lower or equal proportions of pS16 with respect to pS1368 were not sufficient to displace pS1368 from $Th_2pS1368_2$ and pS16 proportion higher than pS1368 led to the formation of a predominant ternary complex $Th_2(pS16)(pS1368)$, demonstrating preferential Th^{4+} binding to the tetra-phosphorylated peptide. Finally, online identification and quantification of the formed complexes when Th^{4+} and UO_2^{2+} were mixed in equimolar ratio relatively to pS1368 showed that in spite of pS1368 has been specifically designed to coordinate UO_2^{2+}, pS1368 is also Th^{4+}-selective and exhibits stronger affinity for this latter than for UO_2^{2+}. Hence, the results gathered through this approach highlight the impact of Th^{4+} coordination chemistry on its interaction with pS1368 and more widely to its affinity for biomolecules.

1. Introduction

Since its introduction by Alpert in the nineteen's [1], hydrophilic interaction liquid chromatography (HILIC) has been widely exploited in numerous fields such as biomedical, biopharmaceutical, metabolomics, proteomics or food sector [2–4]. Numerous reviews focusing on the wide application range of HILIC in bioanalysis [5,6] and on fundamentals of its complex separation mechanism have been reported [7,8]. Although HILIC features are greatly relevant to separate polar metallic complexes, the use of this separation mode has been less described in speciation analysis or metallomics fields, except for the analysis of gadolinium derivatives which are of great interest as contrast agents for medical imaging [9–12].

In previous works, we took advantage of HILIC to separate for the first time uranyl (UO_2^{2+}) complexes with biomimetic peptides, of interest in nuclear toxicology [13,14]. Biomimetic approaches based on synthetic peptides as models of proteins are powerful to characterize protein's coordination sites responsible for the high affinity towards UO_2^{2+}

* Corresponding author.
E-mail address: carole.bresson@cea.fr (C. Bresson).
[1] Present address: Department of Chemistry, Ghent University, Krijgslaan 281-S12, 9000 Ghent, Belgium

https://doi.org/10.1016/j.chroma.2024.465341
Received 24 July 2024; Received in revised form 2 September 2024; Accepted 3 September 2024
Available online 3 September 2024

and to better understand the toxicity mechanisms of this actinide (An) at the molecular scale [15]. These approaches are also highly relevant to provide primary molecular structures for the development of selective chelating agents for decorporation. Following this strategy, a series of multi-phosphorylated cyclic peptides has been synthesized to model the interaction sites of osteopontin (OPN), a hyper-phosphorylated target protein of UO_2^{2+} [16–19] (Fig. 1).

We also developed a dedicated analytical method based on the simultaneous coupling of HILIC to electrospray ionization mass spectrometry (ESI-MS) and inductively coupled plasma mass spectrometry (ICP-MS), to identify the separated complexes and determine simultaneously the selectivity and the affinity of the different biomimetic peptides towards UO_2^{2+}. Furthermore, the selectivity of the peptide with the highest affinity (pS1368) towards UO_2^{2+} was determined in the presence of competing cations such as Cu^{2+}, Zn^{2+} and Sr^{2+} by applying this new method [13,14].

Plutonium (Pu) is another major element in the nuclear sector recently experiencing a resurgence and in case of contamination, Pu is suggested to occur *in vivo* mainly in the form of Pu(IV) species [20]. The thorough knowledge of Pu^{4+} interaction sites in target proteins is required to shed light on its toxicity mechanisms at the molecular level and to be able to develop specifically tuned decorporating agents. The interaction sites of Pu^{4+} in proteins should be similar as those of UO_2^{2+} as they both behave as hard acids according to the Pearson classification, with a significant affinity towards hard bases and particularly towards phosphate groups [21]. *In vivo*, UO_2^{2+} and Pu^{4+} may then compete to interact with coordination sites of proteins playing a major role in the accumulation of An. To date, some works investigating structural or thermodynamic information on Pu(IV)-complexes containing proteins such as fetuin, transferrin, calmodulin or ferritin have been reported in the literature by using techniques such as X-Ray absorption or infra-red spectroscopy as well as capillary electrophoresis coupled to ICP-MS [22–27]. However, further research regarding the potential competition of Pu^{4+} and UO_2^{2+} to interact with target biomolecules is still lacking, particularly with OPN. Investigating the behavior of these An when they are both in presence of phosphorylated biomimetic peptides is therefore essential.

In the present work, we extended the HILIC-ESI-MS/ICP-MS approach that we previously developed, to investigate the affinity of pS16/pS1368 phosphorylated peptides towards Th^{4+}. This latter was selected as a Pu^{4+} analogue to carry out the studies in a conventional laboratory as both An are hard Lewis acids, display the same oxidation state and show high affinity for ligands containing hard donor atoms [21]. Moreover, the charge densities of Th^{4+} and Pu^{4+}, expressed by the charge-to-ionic radius ratio, are in the same range: 3.8 e.$Å^{-1}$ (Th^{4+}) and 4.2 e.$Å^{-1}$ (Pu^{4+}) for the same coordination number (CN=8) [28]. The aim was also to evaluate the selectivity of the most powerful peptide, pS1368, towards Th^{4+} in presence of UO_2^{2+} as competing ion. The methodology was developed according to the following steps: i) evaluation of the selectivity of several polar HILIC stationary phases for separating Th^{4+}-peptide complexes at physiological pH 7.4, reflecting relevant biological conditions in toxicology, ii) determination of the quantitative distribution of Th^{4+} among the pS16/pS1368 separated complexes owing to their simultaneous online identification and quantification, to assess the relative affinity of the two peptides for Th^{4+}, iii) online determination of the quantitative distribution of Th^{4+} and UO_2^{2+} among the pS1368 complexes, to estimate the mutual influence of these An on their complexation properties and the selectivity of pS1368.

This study highlights the tremendous potential of HILIC to separate hydrophilic polar analytes such as An complexes, which are known for their complex chemistry and to be involved in electrostatic interactions upon coordination, rendering the task of their separation very difficult while preserving their integrity. This opens the door to a better knowledge of An behavior at the molecular scale, which is not generally achievable using separation modes commonly encountered in the literature. This is of prime concern in the field of nuclear toxicology, to better understand the An toxicity mechanisms and further develop specific decorporating agents

2. Experimental part

2.1. Chemicals

Acetonitrile (ACN, CH_3CN, LC-MS grade) and ammonia NH_3 (20–22 %) were purchased from VWR prolabo (Briare le canal, France). Ammonium acetate ($NH_4CH_3CO_2$) and toluene ($C_6H_5CH_3$, purity >

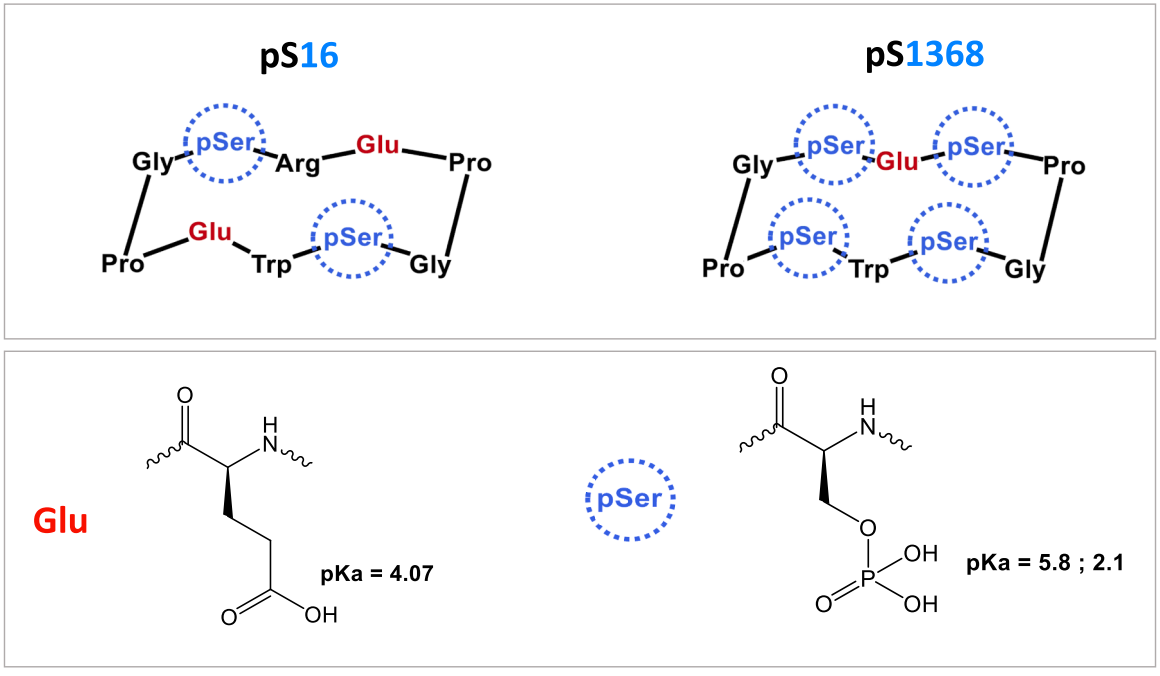

Fig. 1. Structure of the di-and tetra-phosphorylated cyclic peptides pS16 and pS1368 synthesized according to a biomimetic approach and typical pKas of glutamate and phosphoserine side chains.

99.7%) were supplied by Sigma Aldrich (Saint Quentin Fallavier, France). Thorium (Th), uranium (U) and bismuth (Bi) standard solutions (1000 µg mL^{-1}) in HNO_3 2% *w/w*, were provided by the SPEX Certiprep Group (Longjumeau, France). Diethylene triamine pentaacetic acid (DTPA, $C_{14}H_{23}O_{10}N_3$, purity ≥ 98 %) was provided by Sigma Aldrich (Saint Quentin Fallavier, France). L-Tryptophan (Trp) (99 % purity) was purchased from Acros Organics. Nitric acid solutions (HNO_3 2% *w/w*) were prepared by diluting in ultrapure water, HNO_3 65 % (Merck, France) which was distilled with evapoclean from Analab (France). Ultrapure water (18.2 MΩ cm at 25 °C) was obtained from Milli-Q purification system (Merck millipore, Guyancourt, France).

Cyclic di-phosphorylated peptide pS16 was synthetized, characterized and supplied by the CIBEST team at SyMMES (Univ. Grenoble Alpes, CEA, CNRS, Grenoble INP, IRIG, 38 000 Grenoble - France) following the procedures described elsewhere [16]. Cyclic tetra-phosphorylated peptide pS1368 was supplied by Cambridge peptides (Cambridge, UK) following the procedure developed by the CIBEST team [18].

2.2. Preparation of stock solutions and samples

2.2.1. Uranium, thorium and peptide stock solutions

The natural uranium stock solution was prepared by diluting in ultrapure water an in-house U_{nat} solution [29] which was prepared in 0.5 mol L^{-1} ultrapure HNO_3, to achieve a U_{nat} concentration of 10,000 µg mL^{-1} (5×10^{-2} mol L^{-1}). The U_{nat} concentration was measured by ICP-MS, based on external calibration and was 9447.2 µg mL^{-1} (3.97×10^{-2} mol L^{-1}).

Thorium stock solution was prepared by evaporating to dryness 10 mL of the standard solution on a hot plate at 95 °C, and further recovering the residue with 1 mL of 2 % HNO_3 to achieve a Th concentration of 10,000 µg mL^{-1}. The Th concentration was measured by external calibration using ICP-MS and was 9496.4 µg mL^{-1} (4.09×10^{-2} mol L^{-1}).

The peptide stock solutions were prepared by dissolving the adequate amount of the targeted peptide powder in 20 mmol L^{-1} of $NH_4CH_3CO_2$ (pH ~ 7.4) to reach a concentration between 2 and 4 mmol L^{-1}. The concentration of the peptides was determined by external calibration, using HILIC coupled to UV/VIS in series with ESI-MS, by quantifying the Trp contained in the sequence of all peptides (UV absorption at λ = 280 nm). Trp standard solutions were obtained by diluting in 70/30 ACN/H_2O *v/v* containing 20 mmol L^{-1} $NH_4CH_3CO_2$, a Trp solution of 10^{-2} mol L^{-1} prepared in 20 mmol L^{-1} $NH_4CH_3CO_2$, to reach concentrations that ranged between 5×10^{-6} mol L^{-1} and 2×10^{-4} mol L^{-1}.

2.2.2. Preparation of the samples

Th^{4+} in presence of pS16 and pS1368 (2Th:xpS16:ypS1368): in a first step, contact solutions containing several Th:peptide ratios were prepared by adding a very small volume (around 1.5 µL) of Th stock solution in 125–250 µL of peptide stock solutions, to obtain Th concentration ranging between 2 and 5×10^{-4} mol L^{-1}. The pH was adjusted to 7.4 by using ammonia (20–22 %). The concentration of the peptides in these contact solutions was determined by weight, while taking into account the concentration of the peptide stock solution. The contact solutions were systematically prepared the day before the analysis. Finally, the working samples were freshly prepared before analysis by diluting the contact solutions by a factor of 5 in the adequate mobile phase volume, to reach a final Th concentration of 10^{-4} mol L^{-1}. Th was quantified by ICP-MS in each sample and the experimental Th:peptide ratios determined (Table 1).

Th^{4+} and UO_2^{2+} in competition for pS1368 complexation (1Th:1UO_2:2pS1368): the corresponding contact solution was prepared by adding 1.5 µL of each Th and U stock solutions in 125 µL of pS1368 stock solution, to reach a final concentration of 5×10^{-4} mol L^{-1} for both U and Th. Finally, the contact solution was diluted by a factor of 5 in the adequate mobile phase volume, to reach a final An concentration of 10^{-4} mol L^{-1}.

2.3. Instrumentation

2.3.1. Hydrophilic interaction liquid chromatography

Experiments were carried out using an ultimate 3000 UHPLC$^+$ Dionex/Thermofisher scientific (Courtaboeuf, France), made of a degasser, a dual RS pump, an RS autosampler, a column compartment and an RS diode array detector. The columns used in this study are Acquity BEH Amide (150×2.1 mm; 1.7 µm, Waters), Acquity BEH HILIC (150×2.1 mm; 1.7 µm, Waters) and ZIC—HILIC (150×2.1 mm, 3.5 µm, Merck). The composition of the desired mobile phase was obtained by online mixing in the adequate proportions, solvent A (60/40 ACN/H_2O *v/v* containing 20 mmol L^{-1} $NH_4CH_3CO_2$) and solvent B (80/20 ACN/H_2O *v/v* containing 20 mmol L^{-1} $NH_4CH_3CO_2$).

For the quantification of pS16 and pS1368 in the stock solutions, an YMC Triart diol (100×2 mm; 1.9 µm) column was used with a mobile phase composed of 70/30 ACN/H_2O *v/v* and 20 mmol L^{-1} $NH_4CH_3CO_2$, eluting in isocratic mode at 300 µL min^{-1} and the injection volume was 3 µL.

The retention factor *k* of the analytes was calculated following the Eq. (1):

$$k = \frac{(t_R - t_0)}{t_0} \quad (1)$$

Where t_R is the retention time (min) of the analyte, determined by HILIC-ESI-MS, t_0 is the void time of the toluene as unretained marker (10^{-4} mol L^{-1}, V_{inj} = 1 µL), determined by HILIC-UV/VIS at λ = 254 nm.

The resolution factor R_s of the separations was calculated based on the Eq. (2):

$$\mathbf{Rs} = 1.18\ \mathbf{x}\ \frac{\boldsymbol{t_{R2} - t_{R1}}}{\boldsymbol{W_{0.5h1} + W_{0.5h2}}} \quad (2)$$

With analyte 2 more retained than analyte 1. $W_{0.5}$ corresponds to full width half-maximum of each peak.

2.3.2. Mass spectrometers

The used ESI mass spectrometers were a TSQ Quantum Ultra (Thermo Fisher Scientific, San Diego CA, USA) with a triple quadrupole mass analyzer (QqQ) and a LTQ Velos Pro (Thermo Fisher Scientific, San Diego CA USA) with a linear ion trap (LIT) analyzer. The ionization source of both mass spectrometers was equipped with an H-ESI-II probe.

Table 1
Concentration of Th, pS16 and pS1368 determined in the samples and corresponding experimental ratios *2Th:xpS16:ypS1368*. For simplification, the samples associated to each ratio were assigned by a letter (A-E).

Sample	Targeted ratio *2Th:xpS16:ypS1368*	$[Th]_{total}$ µg mL^{-1} (mol L^{-1})	[peptide] mol L^{-1}		Experimental ratio *2Th:x pS16:ypS1368*
			pS16	pS1368	
A	2:0:4	27.30 (1.18×10^{-4})	0.0	2.02×10^{-4}	2:0:3.4
B	2:1:3	33.26 (1.43×10^{-4})	5.12×10^{-5}	2.12×10^{-4}	2:0.7:3
C	2:2:2	33.67 (1.45×10^{-4})	1.10×10^{-4}	1.25×10^{-4}	2:1.5:1.7
D	2:3.5:0.5	17.84 (7.69×10^{-5})	1.88×10^{-4}	2.63×10^{-5}	2:4.9:0.7
E	2:4:0	21.90 (9.44×10^{-5})	1.88×10^{-4}	0.0	2:4:0

All mass spectra were recorded in negative ionization mode. For the sake of clarity, the $Th^{4+}$and UO_2^{2+} complexes were denoted along the manuscript Th_2(peptide)$_2$ or UO_2(peptide), by omitting the charge.

For the study of the complexes in solution by using the ESI-LIT-MS, the samples were continuously introduced into the source at a flow rate of 10 μL min^{-1}. For the chromatographic experiments by coupling HILIC to ESI-QqQ-MS or ESI-LIT-MS, the flow introduced into the source was 300 μL.min^{-1}. In all cases, the source parameters applied for each mass spectrometer are presented in Table 2.

For the ESI-QqQ-MS, chromatograms were extracted from the total ionic current (TIC) and the mass spectra were acquired in full scan mode (*m/z* 600–1500) and in single ion monitoring (SIM) mode, by selecting the *m/z* ratio of highest abundance of the free peptides and An(peptide) complexes (spectral width: ± 0.5 *m/z*). For the ESI-LIT-MS, mass spectra obtained by direct injection of the samples were recorded in full scan mode (*m/z* 600–1700) and in zoom scan mode, by centering the *m/z* ratio on 980 and 1470 for Th^{4+} complexes of pS16 and 1012 and 1519 for Th^{4+} complexes of pS1368. For coupling experiments, chromatograms were extracted from the TIC, by selecting *m/z* ratio of the highest abundance for each analyte.

The ICP-MS instrument was a single quadrupole XSeriesII (Thermo Fisher Scientific, San Diego, USA). The sample introduction system consisted of a perfluoroalkoxy PFA-ST nebulizer operating at 200 μL min^{-1} followed by a quartz cyclonic spray chamber thermostated at 3 °C (PC3 system from Elemental Scientific Instruments, Hoenheim, France). The simultaneous coupling of HILIC to ESI-QqQ-MS and ICP-MS was performed according to the setting up described in our previous work [30]. In order to prevent any carbon deposition due to the use of organic solvents, additional 8 mL min^{-1} oxygen flow rate was introduced in the plasma, through an "additional gas port" located in the spray chamber [31,32]. A platinum skimmer, a sampler cone and a 1 mm inner diameter injector were additionally used for this purpose. The chromatograms were recorded based on the signals of $^{232}Th^+$, $^{238}U^+$ and $^{209}Bi^+$ with an integration time of 90 ms for each isotope.

2.4. Quantitative distribution of Th^{4+} and UO_2^{2+} among the separated complexes

The method previously developed for online quantification of UO_2^{2+} by ICP-MS [13,14] was used hereby to online quantify the Th^{4+} complexes coming from the HILIC separation. Firstly, all of thorium $[Th]_{total}$ was quantified in each sample using external calibration, by introducing the sample in flow injection analysis mode (FIA). Secondly, the samples were injected in duplicate into the column. The Th^{4+} complexes were then separated, online identified by ESI-MS and simultaneously quantified by ICP-MS as [Th(peptide)], based on the total integration of the corresponding chromatographic peaks combined to external calibration. The free Th^{4+} fraction potentially adsorbed on the column was desorbed owing to injections of DTPA solution at 5×10^{-4} mol L^{-1} and the sum of the areas of the peaks allowed to quantify the total free Th^{4+} fraction, as [Th(free)].

The quantitative distribution of Th^{4+} among its different chemical forms, expressed in percent (%), was calculated following Eq. (3):

$$\%\ \mathrm{Th(X)} = \frac{[Th(X)]}{[Th]total} \quad (3)$$

With X = peptide or free

For competition experiments of UO_2^{2+} and Th^{4+} towards pS1368 complexation, the relative quantitative distribution of these An among the formed pS1368 complexes was calculated as the ratio of the area of the chromatographic peak of each complex and the area of the peak associated to the totality of the species of the considered An, obtained by introducing the sample in FIA mode, following Eq. (4):

$$\%\ \mathrm{An(pS1368)} = \frac{Peak\ area\ An(pS1368)}{Peak\ area\ An\ total} \quad (4)$$

With An = Th or UO_2.

Table 2
ESI source parameters selected for both instruments in (A) HILIC coupling and (B) direct introduction of the samples.

	ESI-QqQ-MS (A)	ESI-LIT-MS	
		(A)	(B)
Spray voltage (V)	−3540	−3500	−3500
Source heater temperature (°C)	120	120	90
Capillary temperature (°C)	360	380	280
Sheath gas flow (arbitrary unit)	40	45	20
Auxiliary gas flow (arbitrary unit)	15	20	10
Skimmer offset (V)	0	/	/
S lens (%)	/	70	70

3. Results and discussion

3.1. Characterization of Th^{4+}-peptide complexes in solution by ESI-LIT-MS

The coordination chemistry of Th^{4+} is various and unique, with high coordination numbers (up to 12 or 15), leading to the complexation of a wide range of ligands and often the formation of oligomeric complexes [33]. The first mandatory step consisted then in the characterization of the formed complexes in solution, resulting from the addition of two equivalents of the peptides to one equivalent of Th^{4+} at pH around 7.4. This step was carried out by ESI-LIT-MS used in direct introduction mode and mass spectra are shown in Fig. 2.

From the mass spectra recorded in full scan mode, Th_2(peptide)$_2$ dimeric complexes were identified as the main formed species for pS16 and pS1368 (Fig. 2A and B). Experiments further carried out in zoom scan mode to detect isotopic patterns with higher resolution, allowed to confirm the Th_2(peptide)$_2$ stoichiometry for both complexes and the presence of di- and tri-charged forms $[Th_2(peptide)_2–10H]^{2-}$ and $[Th_2(peptide)_2–11H]^{3-}$ (see insets Fig. 2). In all cases, the charge of these newly characterised complexes is in line with the known +IV oxidation state of thorium.

Interestingly, UO_2^{2+} monomeric complexes of 1:1 stoichiometry were predominantly formed by reaction with one equivalent of pS16 or pS1368 at pH ~ 7.4 [16–18]. In fact, these cyclic peptides have been specifically designed to promote the coordination of the four amino acid's side-chains (Glu and pSer, see Fig. 1) in the equatorial plane of UO_2^{2+}, therefore favouring the 1:1 complex in stoichiometric conditions. However, complexes of 2:1 stoichiometry were preferred in excess of UO_2^{2+} relatively to pS16 or pS1368, as the coordination of a second UO_2^{2+} cation being favoured because of its large affinity for phosphate groups. When UO_2^{2+} was present at lower concentration relative to the peptides, a complex of 1:2 stoichiometry, exhibiting a very low stability was also evidenced only with pS1368 [16]. By contrast to UO_2^{2+} interacting with four to six atoms in its equatorial plane, only, Th^{4+} coordination is known to be spherical with large coordination numbers. Therefore, the formation of the dimeric complexes Th_2(peptide)$_2$ most likely fulfils the requirements for spherical geometry through high coordination number, including bridging phosphates, around the two Th^{4+} cations. The different properties of these An are thus likely responsible for the different stoichiometry and nuclearity of the associated complexes.

3.2. HILIC retention behavior of the Th^{4+}-peptide complexes

In order to evaluate the impact of the phosphorylation degree of the peptides on their affinity for Th^{4+}, the corresponding complexes must be first separated with a good selectivity and baseline resolution. Since Th-pS1368/Th-pS16 complexes are polar and charged, we investigated different chromatographic conditions in the aim of separating them at pH ~ 7.4. This task was carried by coupling HILIC to ESI-LIT-MS, to

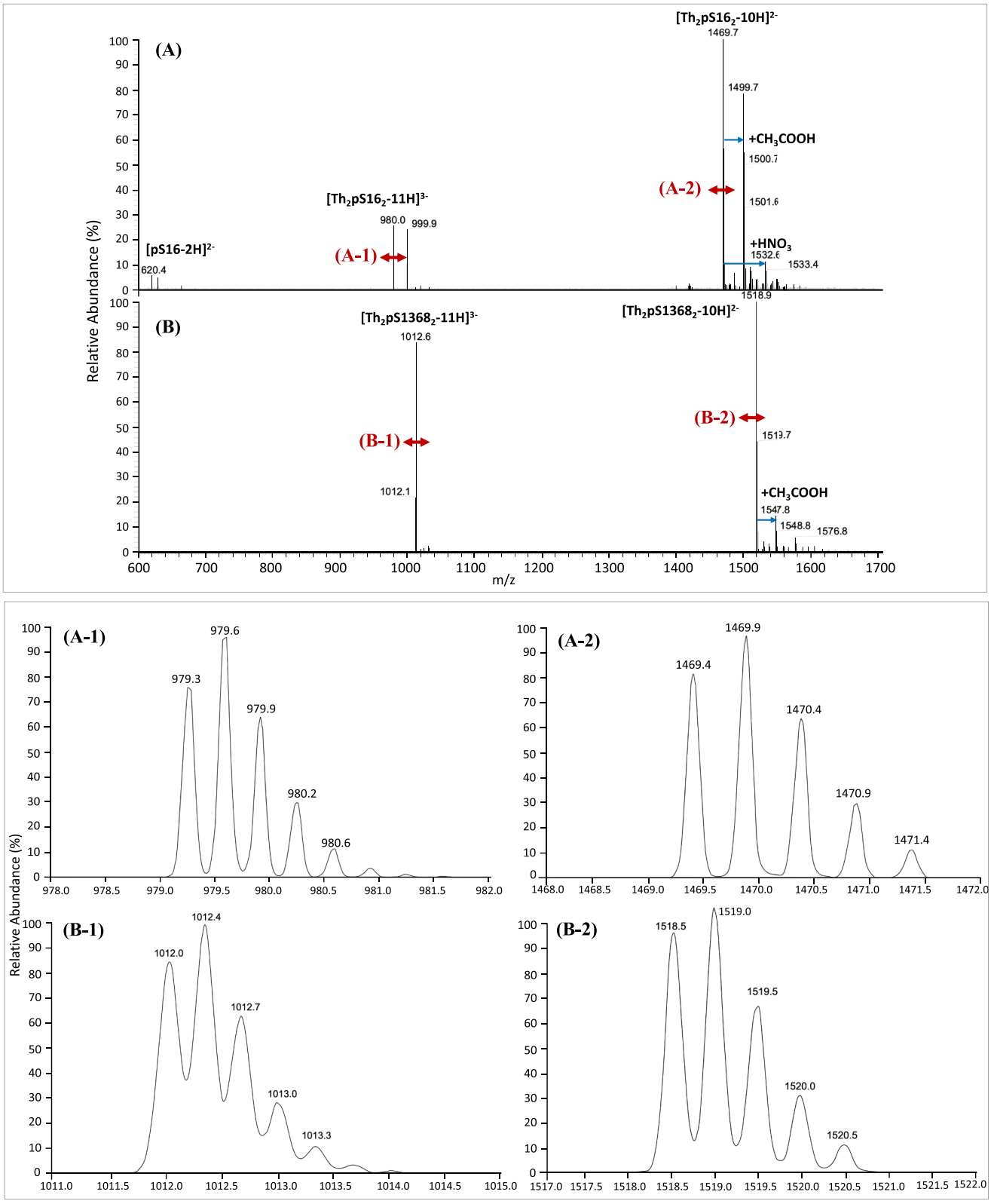

Fig. 2. Full scan ESI mass spectra of Th-pS16 (A) and pS1368 (B) complexes at pH ~ 7.4 recorded in negative ionisation mode. Insets: mass spectra of Th-pS16 (A1 and A2) and pS1368 (B1 and B2) complexes, recorded in zoom scan mode. Samples were prepared in 70/30 ACN/H_2O *v/v* and 20 mmol L^{-1} $NH_4CH_3CO_2$ with [Th] = 10^{-4} mol L^{-1}.

identify each complex and their retention factor, following independent injections of the complexes into the column. The selectivity of non-grafted hybrid silica (BEH HILIC), amide (BEH amide) and zwitterionic-grafted (ZIC—HILIC) stationary phases was evaluated and the elution profiles of the complexes are overlaid in Fig. 3, for a mobile phase composed of 70/30 ACN/H_2O *v/v* and 20 mmol L^{-1} $NH_4CH_3CO_2$.

As shown in Fig. 3, the Th^{4+} complex of pS1368 is systematically more retained on the three columns than the pS16 complex, while this

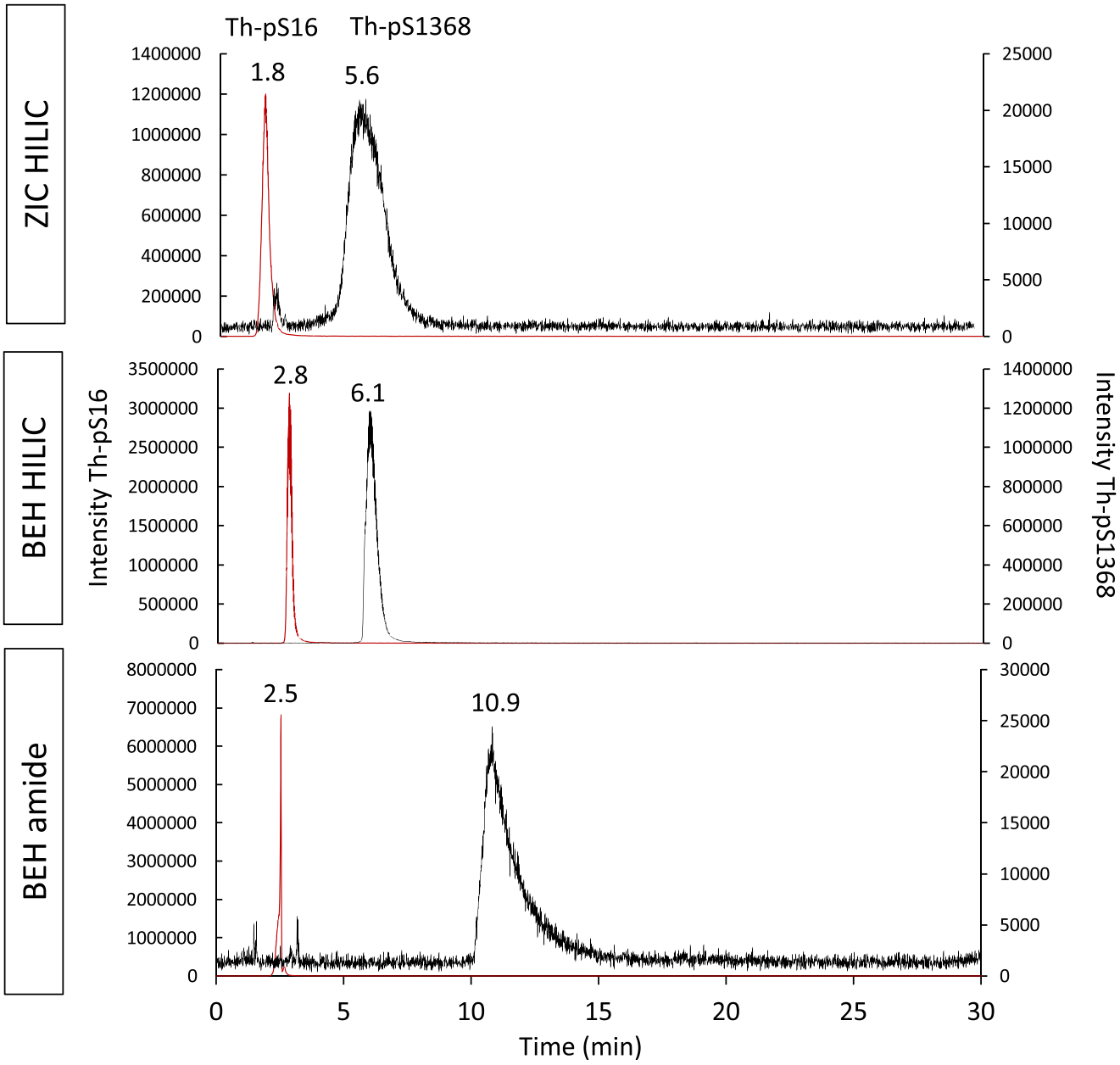

Fig. 3. Overlay of the extracted ion current elution profiles of Th-pS16 (red) and pS1368 (black) complexes, acquired by ESI-LIT-MS, with *m/z* 1469–1470 and 1518–1520 for Th_2pS16_2 and $Th_2pS1368_2$, respectively. Samples: 1Th:2pS16 (Sample E) and 1Th:2pS1368 (Sample A). Columns: ZIC—HILIC 150 × 2.1 mm, 3.5 μm, Acquity BEH HILIC 150 × 2.1 mm, 1.7 μm and Acquity BEH AMIDE 150 × 2.1 mm; 1.7 μm. In all cases, the mobile phase composition was 70/30 ACN/H_2O *v/v* containing 20 mmol L^{-1} $NH_4CH_3CO_2$, the flow rate was 300 μL min^{-1}, the elution mode isocratic and V_{inj} = 3 μL.

latter is poorly retained despite the differences in the polarity and charge of the grafted chemical groups. The retention factor of Th-pS16 complex displayed small changes, being 0.8, 1.5 and 1.8 for ZIC—HILIC, BEH amide and BEH HILIC, respectively. On the other hand, the retention factor of Th-pS1368 increased in the following order for the columns: ZIC—HILIC < Acquity BEH HILIC < Acquity BEH amide, being 4.7, 5.2 and 10, respectively.

The behavior of the Th-pS16 complex is quite puzzling since it exhibits globally a weak retention on the three columns. First of all, upon complexation with Th^{4+}, the maximum overall charge of pS16 decreases from −5 to −2 for dimeric complex at neutral pH, leading to decreased retention according to the classical hydrophilic partitioning [34]. In addition, secondary electrostatic or hydrogen bonding interactions do not seem to participate significantly to the retention process, in particular for the ZIC—HILIC column, as Th-pS16 eluted close to the dead-time. These observations confirm the complexity of the HILIC retention mode and the challenge to predict a compound's behavior. Much mechanistic investigations still need to be done to understand the HILIC behaviour of metallic complexes, which will be useful in several fields of applications.

As mentioned previously, Th-pS1368 complex is more retained than Th-pS16 on the three columns, with retention factors higher than 4. This is in accordance with the higher polarity/charge of −10 for the dimeric complexes formed with the tetra-phosphorylated peptide pS1368 in comparison with those formed with the di-phosphorylated peptide pS16, as the former peptide displays two additional negatively charged phosphorylated groups in its scaffold. Moreover, pS1368 displays a negatively charged glutamate (Glu) in position 2 of the peptide scaffold, while pS16 contains a positively charged arginine (Arg) in the same position (see Fig. 1), which tends to further reduce the global negative

charge of Th-pS16 complexes. This allows to suggest that the retention of Th-pS1368 complexes obey to hydrophilic partitioning as predominant mechanism, but additional hydrogen bonding interactions seem to take an important part, particularly for the Acquity BEH amide column as the retention factor increased by almost 2-fold in comparison with the other columns. These results are in line with what we previously observed when optimizing the HILIC separation conditions of a series of biomimetic peptides [34] and complexes of UO_2^{2+} and lanthanides containing different ligands [30,35,36], using several stationary phases.

Overall, Th^{4+} complexes of pS16 and pS1368 can be successfully separated using three stationary phases of different functionalization, with resolution factors of 7.8, 6.1 and 2.3 for BEH HILIC, BEH amide and ZIC—HILIC, respectively. The Acquity BEH HILIC column with a mobile phase composed of 70/30 ACN/H_2O *v/v* and 20 mmol L^{-1} $NH_4CH_3CO_2$ was then preferred for the rest of our study, as these are the best conditions to separate both complexes with the highest resolution factor and the most satisfying peak shapes. In these conditions, dimeric $Th_2(pS16)_2$ and $Th_2(pS1368)_2$ complexes were detected with the highest abundance, in agreement with the stoichiometry of the complexes observed by using direct injection mode. This also show that the dimeric structure of the complexes was preserved for both peptides through HILIC separation.

3.3. Determination of the relative affinity of the peptides towards Th^{4+} using HILIC-ESI-MS/ICP-MS

Like the other An, Th^{4+} exhibits high affinity for phosphate groups [37] and one promising decorporating agent of Th^{4+} recently described in the literature contain several phosphorylated functions [38–40]. Furthermore, the Th^{4+} interaction with OPN was demonstrated to be dominated by two oxgen atoms from phosphate groups binding to the An cation [41]. Therefore, the phosphorylation degree of the biomimetic peptides is expected to play a pivotal role in their affinity for Th^{4+}. In order to evaluate the impact of this key parameter, several ratios of the di- and tetra-phosphorylated peptides, pS16 and pS1368, were added in a competing complexation reaction towards Th^{4+} (*2Th:xpS16:ypS1368*) at pH ~ 7.4. The formed complexes were separated using HILIC, online identified by ESI-MS and simultaneously quantified by ICP-MS in a single step, following the method developed in our previous work [13]. The overlay of the chromatograms acquired by ICP-MS for samples A-E (Table 1) is presented in Fig. 4.

As shown in Fig. 4, a single peak with a retention factor of 1.8 was detected when only pS16 was added to Th^{4+} (Sample E). By comparing this retention factor with the one obtained using ESI-MS, the peak was attributed to $Th_2(pS16)_2$. A peak tailing was observed, which could possibly be related to the formation of additional Th-containing species. Unfortunately, the extraction of the ESI mass spectrum from the tailing did not reveal the structural identity of this species. For samples A to C, containing excess or equal ratio of pS1368 relatively to pS16, only the peak of $Th_2(pS1368)_2$, attributed owing to ESI-MS, was detected (Fig. 4). This means that even when pS16 is present in equivalent ratio as pS1368, it does not displace pS1368 from $Th_2(pS1368)_2$, which strongly supports a higher affinity of pS1368 towards Th^{4+} with respect to pS16. Furthermore, when pS16 is in excess in comparison with pS1368 (Sample D), two peaks were observed in addition to those corresponding to $Th_2(pS16)_2$ and $Th_2(pS1368)_2$. The peak with a retention factor of 2.8 was attributed to a ternary binuclear complex $Th_2(pS16)(pS1368)$, after matching its retention factor with this of the peak detected by ESI-MS, while the remaining peak eluting at $k = 3.5$ could not be attributed. The occurrence of this ternary complex is in accordance with a previously published work, reporting Th^{4+} ternary binuclear complex formed with Transferrin (Tf) and an iron biding siderophore Deferoxamine (DFOB), as $Th_2(Tf)(DFOB)$ [27].

As the species contained in the Sample D could not be separated with baseline resolution, a peak deconvolution was performed in order to estimate the surface area of each peak and further deduce the quantitative distribution of Th^{4+} within the different species by applying Eq. (3). The proportion of the Th species (%) determined for each sample is shown in Fig. 5.

As can be seen in Fig. 5, when Th^{4+} is in presence of pS1368 solely or in higher/equimolar proportion with respect to pS16, it is fully bound to pS1368 (Samples A-C). When Th^{4+} is in the presence of pS16 only (Sample E), 92% of total thorium was recovered from the column and distributed as follows: 64 % in $Th_2(pS16)_2$ while 28 % was adsorbed on the column, presumably under free form Th^{4+}. When seven times more pS16 than pS1368 is added to Th^{4+} (Sample D), 94 % of total thorium was recovered from the column and distributed as follows: 19 % in $Th_2(pS16)_2$, 37 % in the ternary complex $Th_2(pS16)(pS1368)$, 9 % in $Th_2(pS1368)_2$, 21 % was under free Th^{4+} form and 8 % unidentified.

These results allow to demonstrate that Th^{4+} coordinates

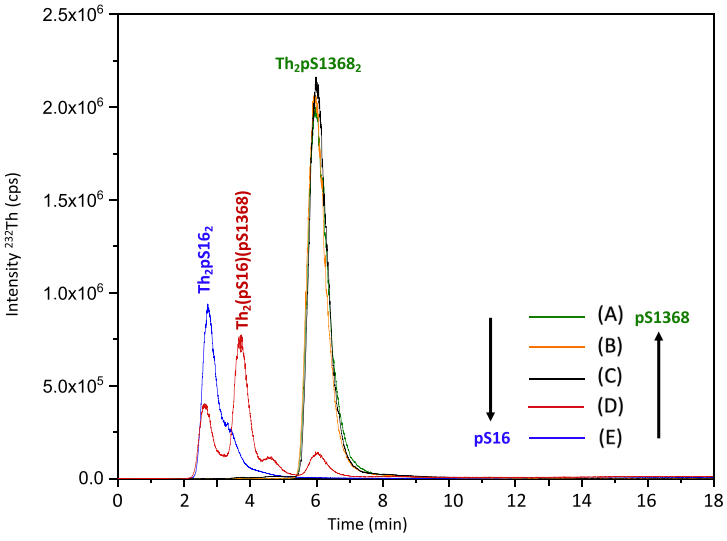

Fig. 4. Overlay of the chromatograms acquired by ICP-MS, recording the $^{232}Th^+$ signal with an integration time of 90 ms for samples (A-E). 2Th:0pS16:3.4pS1368 (Sample A), 2Th:0.7pS16:3pS1368 (sample B), 2Th:1.5pS16:1.7pS1368 (sample C), 2Th:4.9pS16:0.7pS1368 (sample D), and 2Th:4pS16:0pS1368 (Sample E). Column: Acquity BEH HILIC 150 × 2.1 mm; 1.7 µm. Mobile phase: 70/30 ACN/H_2O *v/v* containing 20 mmol L^{-1} $NH_4CH_3CO_2$. Flow rate: 300 µL min^{-1}, isocratic elution and V_{inj}: 3 µL. Each sample was injected in duplicate.

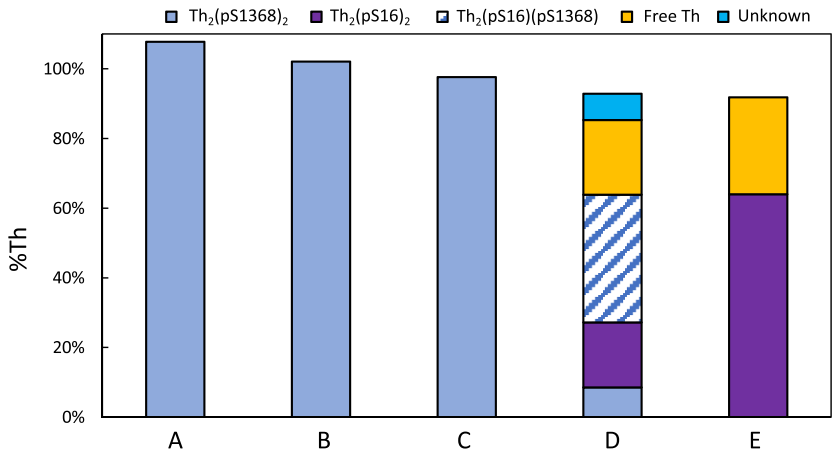

Fig. 5. Quantitative distribution of Th^{4+} expressed in percentage (%) within the different species in samples (A-E), corresponding to the addition of different ratios of pS16 and pS1368 to fixed concentration of Th^{4+} *(2Th:xpS16:ypS1368, see Table1)*. Each sample was analysed in duplicate. The relative error for two measurement replicates for each sample was: (A) 0.8 %, (B) 0.8 %, (C) 5.8 %, (D) 4 % and (E) 2.8 %.

preferentially the tetra-phosphorylated peptide pS1368 compared to the di-phosphorylated one, as previously observed for UO_2^{2+} [13]. The affinity enhancement when the peptide's phosphorylation degree increases from pS16 to pS1368 is in line with the very high affinity of the hard An cations, either UO_2^{2+} or Th^{4+}, for phosphate groups.

3.4. Selectivity and relative affinity of the cyclic tetra-phosphorylated peptide pS1368 for Th^{4+} in presence of UO_2^{2+} as competing ion

As Pu^{4+} and UO_2^{2+} are likely to compete for the coordination with target molecules in the event of internal contamination, we extended the methodology that we developed to determine online and in a single step, the selectivity of pS1368 for Th^{4+} when in presence of UO_2^{2+}. To this end, equimolar ratios of UO_2^{2+} and Th^{4+} were added to two pS1368 equivalents at pH ~ 7.4 (*1Th:1UO_2:2pS1368)*. The simultaneous HILIC-ESI-MS/ICP-MS coupling was applied to identify and quantify the separated formed complexes. The chromatogram obtained by ICP-MS is shown Fig. 6.

First, Fig. 6 clearly shows that the Th^{4+} complex is more retained than the UO_2^{2+} one. This is consistent with the higher polarity of the Th^{4+} species, which has a maximum overall charge of −10 for the dimeric complex Th_2(pS1368)$_2$, higher than the −7 maximum charge of the monomeric complex UO_2(pS1368). As expected, the more polar Th^{4+} species is more retained according to the HILIC retention mode. In addition, the dimeric complex displays two peptides in its structure, potentially available to promote interactions with the polar stationary phase.

Based on the integration of each chromatographic peak, the quantitative distribution of UO_2^{2+} and Th^{4+} among the two complexes was determined according to Eq. (4). It was found that 100 % of Th^{4+} (relative error of 5.2 %, $n = 2$ injections) was in Th_2pS1368$_2$, while only 58 % of UO_2^{2+} (relative error of 0.5 %, $n = 2$ injections) was under the UO_2(pS1368) form, with the remaining fraction presumably retained on the column under the free form UO_2^{2+}. Based on our recent works [13,

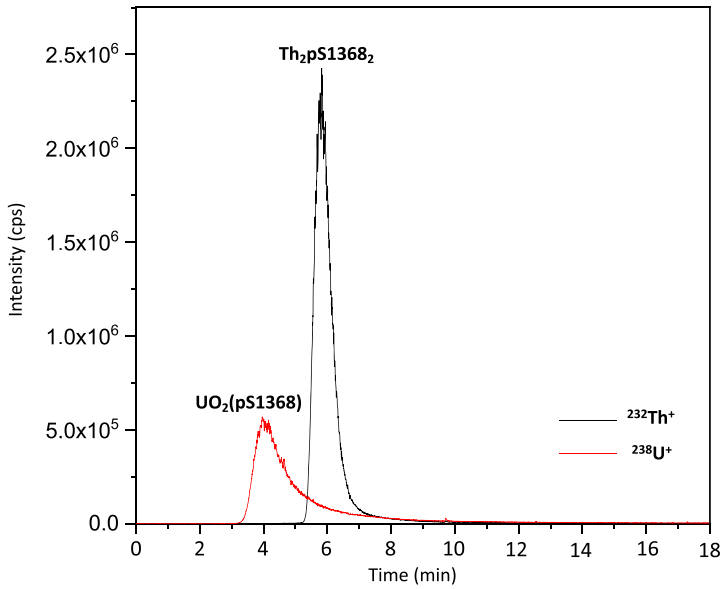

Fig. 6. Chromatogram acquired by ICP-MS, recording the $^{232}Th^+$ and $^{238}U^+$ signals with an integration time of 90 ms. Sample: 1Th:1UO_2:2pS1368. Column: Acquity BEH HILIC 150 × 2.1 mm; 1.7 µm. Mobile phase: 70/30 ACN/H2O *v/v* containing 20 mmol L^{-1} $NH_4CH_3CO_2$. Flow rate: 300 µL min^{-1}, isocratic elution and Vinj: 3 µL. The sample was injected in duplicate.

14], more than 85 % of UO_2^{2+} was coordinated by adding two equivalents of pS1368. Therefore, the lower proportion of UO_2(pS1368) found in the sample containing the two An cations in equimolar ratios and two pS1368 equivalents, allow to suggest a stronger interaction of pS1368 with Th^{4+} than with UO_2^{2+}.

While coordination properties are key parameters having an impact on the chemistry of an element, we must keep in mind that Th^{4+} and UO_2^{2+} are both An with high affinity for phosphate groups, but they exhibit different charges and oxidation states. In addition, the pre-organized cyclic peptide pS1368 was specifically designed to fulfil the specific coordination requirements of UO_2^{2+}, *i.e.* 4 to 6 hard donor atoms in its equatorial plane. The β-sheet structure of this peptide orients the 4 coordinating groups on one side of an averaged plane, which induces UO_2^{2+} coordination through the 4 phosphate functions in its equatorial plane. This planar structure makes also it possible the formation of a dimer promoting a larger number of phosphate groups around two Th^{4+} cations, to fulfil the coordination requirements of Th^{4+}, *i.e.* a large number of hard donors in a spherical geometry. The formation of the resulting dimeric complex $Th_2pS1368_2$ is probably responsible for the relatively stronger interaction of the cyclic tetraphosphorylated peptide with Th^{4+} with respect to UO_2^{2+}.

4. Conclusion

The HILIC-based approach that we developed allowed to evaluate the relative affinity and selectivity of biomimetic peptides towards An, which is of prime importance to better understand the key parameters driving they coordination with target biomolecules *in vivo* or decorporating agents based on chelation. In particular, the simultaneous coupling of HILIC to ESI-MS and ICP-MS was applied to separate, identify and quantify Th^{4+} complexes containing di-and tetra-phosphorylated cyclic peptides, pS16 and pS1368. The selectivity of several stationary phases was assessed and the Acquity BEH HILIC column with a mobile phase composed of 70/30 ACN/H_2O *v/v* and 20 mmol L^{-1} $NH_4CH_3CO_2$ yielded the best separation of the newly identified dimeric complexes $Th_2(pS16)_2$ and $Th_2(pS1368)_2$. The quantitative distribution of Th^{4+} among the separated complexes was determined online and in a single step, showing that the tetra-phosphorylated peptide pS1368 exhibits stronger affinity for Th^{4+} than the di-phosphorylated one, pS16. The addition of equimolar ratios of pS16 and pS1368 to Th^{4+} led to the formation of only the pS1386-containing complex, while only 19 % of $Th_2(pS16)_2$ was formed when pS16 was seven times in excess compared to pS1368, confirming this result. Finally, through the same approach, the relative affinity and selectivity of pS1368 for the two An cations Th^{4+} and UO_2^{2+} was assessed online. Interestingly, this peptide initially designed to promote UO_2^{2+} coordination in the equatorial plane, binds even more efficiently the spherical Th^{4+} cation, probably because of the ability of this latter to form dimeric species, which fulfils the coordination requirement of this An(IV) ion.

The ongoing development of HILIC stationary phases with decreased dimensions and/or core shell particles, sub-2 μm diameter particles and monolithic materials, offers the opportunity to get further insight into the separation of An species based on this separation mode, while decreasing the consumption of the sample and the waste production. This point is of high concern while dealing with radioelements and highly toxic metals.

CRediT authorship contribution statement

Lana Abou-Zeid: Writing – original draft, Visualization, Validation, Methodology, Investigation, Formal analysis, Conceptualization. **Albert Pell:** Writing – review & editing, Validation, Methodology, Investigation, Conceptualization. **Marina Amaral Saraiva:** Writing – review & editing, Validation, Investigation. **Pascale Delangle:** Writing – review & editing, Supervision, Resources, Conceptualization. **Carole Bresson:** Writing – review & editing, Validation, Supervision, Project administration, Methodology, Investigation, Funding acquisition, Conceptualization.

Declaration of competing interest

The authors declare that they have no known competing financial interests or personal relationships that could have appeared to influence the work reported in this paper.

Data availability

Data will be made available on request.

Acknowledgments

The authors thank Mrs Colette Lebrun for preliminary mass spectrometry experiments on the thorium complexes. The authors would also like to acknowledge the Cross-Disciplinary Program on Instrumentation and Detection of CEA, the French Alternative Energies and Atomic Energy Commission and the Cross-cutting basic research Program (RTA Program) of the CEA Energy Division, for their financial support.

References

[1] A.J. Alpert, Hydrophilic-interaction chromatography for the separation of peptides, nucleic acids and other polar compounds, J. Chromatogr. A 499 (1990) 177–196, https://doi.org/10.1016/S0021-9673(00)96972-3.
[2] T. Ikegami, Hydrophilic interaction chromatography for the analysis of biopharmaceutical drugs and therapeutic peptides: a review based on the separation characteristics of the hydrophilic interaction chromatography phases, J. Sep. Sci. 42 (2019) 130–213, https://doi.org/10.1002/jssc.201801074.
[3] G. Marrubini, P. Appelblad, M. Maietta, A. Papetti, Hydrophilic interaction chromatography in food matrices analysis: an updated review, Food Chem. 257 (2018) 53–66, https://doi.org/10.1016/j.foodchem.2018.03.008.
[4] I. Kohler, M. Verhoeven, R. Haselberg, A.F.G. Gargano, Hydrophilic interaction chromatography – mass spectrometry for metabolomics and proteomics: state-of-the-art and current trends, Microchem. J. 175 (2022) 106986, https://doi.org/10.1016/j.microc.2021.106986.
[5] Q. Sheng, M. Liu, M. Lan, G. Qing, Hydrophilic interaction liquid chromatography promotes the development of bio-separation and bio-analytical chemistry, TrAC Trends Anal. Chem. 165 (2023) 117148, https://doi.org/10.1016/j.trac.2023.117148.
[6] E.A. Stijn Hendrickx, D. Cabooter, Recent advances in the application of hydrophilic interaction chromatography for the analysis of biological matrices, Bioanalysis 7 (2015) 2927–2945, https://doi.org/10.4155/bio.15.200.
[7] Y. Guo, B. Fattal, Relative significance of hydrophilic partitioning and surface adsorption to the retention of polar compounds in hydrophilic interaction chromatography, Anal. Chim. Acta 1184 (2021) 339025, https://doi.org/10.1016/j.aca.2021.339025.
[8] W. Gao, X. Liu, Y. Wang, C. Liang, H. Lian, J. Qiao, Insight into the hydrophilic interaction liquid chromatographic retention behaviors of hydrophilic compounds on different stationary phases, Talanta 219 (2020) 121363, https://doi.org/10.1016/j.talanta.2020.121363.
[9] S. Okabayashi, L. Kawane, N.Y. Mrabawani, T. Iwai, T. Narukawa, M. Tsuboi, K. Chiba, Speciation analysis of Gadolinium-based contrast agents using aqueous eluent-hydrophilic interaction liquid chromatography hyphenated with inductively coupled plasma-mass spectrometry, Talanta 222 (2021) 121531, https://doi.org/10.1016/j.talanta.2020.121531.
[10] L. Schlatt, A. Köhrer, C. Factor, P. Robert, M. Rasschaert, M. Sperling, U. Karst, Mild dissolution/recomplexation strategy for speciation analysis of gadolinium from MR contrast agents in bone tissues by means of HPLC-ICP-MS, Anal. Chem. 93 (2021) 11398–11405, https://doi.org/10.1021/acs.analchem.1c01100.
[11] M. Horstmann, R. Gonzalez de Vega, D.P. Bishop, U. Karst, P.A. Doble, D. Clases, Determination of gadolinium MRI contrast agents in fresh and oceanic waters of Australia employing micro-solid phase extraction, HILIC-ICP-MS and bandpass mass filtering, J. Anal. At. Spectrom. 36 (2021) 767–775. Kars.
[12] D. Clases, M. Sperling, U. Karst, Analysis of metal-based contrast agents in medicine and the environment, TrAC Trends Anal. Chem. 104 (2018) 135–147, https://doi.org/10.1016/j.trac.2017.12.011.
[13] L. Abou-Zeid, A. Pell, M.G. Cortes, H. Isnard, P. Delangle, C. Bresson, Determination of the affinity of biomimetic peptides for uranium through the simultaneous coupling of HILIC to ESI-MS and ICP-MS, Anal. Chim. Acta 340773 (2022), https://doi.org/10.1016/j.aca.2022.340773.
[14] L. Abou-Zeid, A. Pell, M. Garcia-Cortes, H. Isnard, P. Delangle, C. Bresson, Determining the selectivity of a tetra-phosphorylated biomimetic peptide towards uranium in the presence of competing cations through the simultaneous coupling

of HILIC to ESI–MS and ICP-MS, Anal. Bioanal. Chem. (2023), https://doi.org/10.1007/s00216-023-04884-4.
[15] A. Garai, P. Delangle, Recent advances in uranyl binding in proteins thanks to biomimetic peptides, J. Inorg. Biochem. 203 (2020) 110936, https://doi.org/10.1016/j.jinorgbio.2019.110936.
[16] M. Starck, N. Sisommay, F.A. Laporte, S. Oros, C. Lebrun, P. Delangle, Preorganized peptide scaffolds as mimics of phosphorylated proteins binding sites with a high affinity for uranyl, Inorg. Chem. 54 (2015) 11557–11562, https://doi.org/10.1021/acs.inorgchem.5b02249.
[17] M. Starck, F.A. Laporte, S. Oros, N. Sisommay, V. Gathu, P.L. Solari, G. Creff, J. Roques, C. DenAuwer, C. Lebrun, P. Delangle, Cyclic phosphopeptides to rationalize the role of phosphoamino acids in uranyl binding to biological targets, Chem. Eur. J. 23 (2017) 5281–5290, https://doi.org/10.1002/chem.201605481.
[18] F.A. Laporte, C. Lebrun, C. Vidaud, P. Delangle, Phosphate-rich biomimetic peptides shed light on high-affinity hyperphosphorylated uranyl binding sites in phosphoproteins, Chem. A Eur. J. 25 (2019) 8570–8578, https://doi.org/10.1002/chem.201900646.
[19] F. Laporte, Y. Chenavier, A. Botz, C. Gateau, C. Lebrun, S. Hostachy, C. Vidaud, P. Delangle, A simple fluorescence affinity assay to decipher uranyl-binding to native proteins, Angew. Chem. Int. Ed. (2022) 61, https://doi.org/10.1002/anie.202203198.
[20] P.W. Durbin, Actinides in animals and man, L.R. Morss, N.M. Edelstein, J. Fuger (Eds.). The Chemistry of the Actinide and Transactinide Elements, Springer Netherlands, Dordrecht, 2006, pp. 3339–3440, https://doi.org/10.1007/1-4020-3598-5_31.
[21] R.G. Pearson, Hard and soft acids and bases, J. Am. Chem. Soc. 85 (1963) 3533–3539, https://doi.org/10.1021/ja00905a001.
[22] F. Brulfert, J. Aupiais, Topological speciation of actinide–transferrin complexes by capillary isoelectric focusing coupled with inductively coupled plasma mass spectrometry: evidence of the non-closure of the lobes, Dalton Trans. 47 (2018) 9994–10001, https://doi.org/10.1039/C8DT01616J.
[23] C. Vidaud, L. Miccoli, F. Brulfert, J. Aupiais, Fetuin exhibits a strong affinity for plutonium and may facilitate its accumulation in the skeleton, Sci. Rep. 9 (2019) 17584, https://doi.org/10.1038/s41598-019-53770-6.
[24] C. Zurita, S. Tsushima, C. Bresson, M.G Cortes, P.L. Solari, A. Jeanson, G. Creff, C. D Auwer, How does iron storage protein ferritin interact with plutonium (and Thorium)? Chem. A Eur. J. 27 (2021) 2393–2401, https://doi.org/10.1002/chem.202003653.
[25] C. Zurita, S. Tsushima, P.L. Solari, A. Jeanson, G. Creff, C.D Auwer, Interaction of Th(IV), Pu(IV) and Fe(III) with ferritin protein: how similar? J. Synchrotron Radiat. 29 (2022) 45–52, https://doi.org/10.1107/S1600577521012340.
[26] L. Daronnat, V. Holfeltz, N. Boubals, T. Dumas, P. Guilbaud, D.M. Martinez, P. Moisy, S. Sauge-Merle, D. Lemaire, P.L. Solari, L. Berthon, C. Berthomieu, Investigation of the plutonium(IV) interactions with two variants of the EF-hand Ca-binding site I of calmodulin, Inorg. Chem. 62 (2023) 8334–8346, https://doi.org/10.1021/acs.inorgchem.3c00845.
[27] C. Zurita, S. Tsushima, P.L. Solari, D. Menut, S. Dourdain, A. Jeanson, G. Creff, C. D Auwer, Interaction between the transferrin protein and plutonium (and Thorium), What's New? Chem. A Eur. J. 29 (2023) e202300636 https://doi.org/10.1002/chem.202300636.
[28] R.D. Shannon, Revised effective ionic radii and systematic studies of interatomic distances in halides and chalcogenides, Acta Cryst. A 32 (1976) 751–767, https://doi.org/10.1107/S0567739476001551.
[29] E. Paredes, E. Avazeri, V. Malard, C. Vidaud, P.E. Reiller, R. Ortega, A. Nonell, H. Isnard, F. Chartier, C. Bresson, Evidence of isotopic fractionation of natural uranium in cultured human cells, Proc. Natl. Acad. Sci. U. S. A. 113 (2016) 14007–14012, https://doi.org/10.1073/pnas.1610885113.
[30] E. Blanchard, A. Nonell, F. Chartier, A. Rincel, C. Bresson, Evaluation of superficially and fully porous particles for HILIC separation of lanthanide–polyaminocarboxylic species and simultaneous coupling to ESIMS and ICPMS, RSC Adv. 8 (2018) 24760–24772, https://doi.org/10.1039/C8RA02961J.
[31] A. Leclercq, A. Nonell, J.L. Todolí Torró, C. Bresson, L. Vio, T. Vercouter, F. Chartier, Introduction of organic/hydro-organic matrices in inductively coupled plasma optical emission spectrometry and mass spectrometry: a tutorial review. Part I. Theoretical considerations, Anal. Chim. Acta 885 (2015) 33–56, https://doi.org/10.1016/j.aca.2015.03.049.
[32] A. Leclercq, A. Nonell, J.L. Todolí Torró, C. Bresson, L. Vio, T. Vercouter, F. Chartier, Introduction of organic/hydro-organic matrices in inductively coupled plasma optical emission spectrometry and mass spectrometry: a tutorial review. Part II. Practical considerations, Anal. Chim. Acta 885 (2015) 57–91, https://doi.org/10.1016/j.aca.2015.04.039.
[33] C.D. Tutson, A.E.V. Gorden, Thorium coordination: a comprehensive review based on coordination number, Coord. Chem. Rev. 333 (2017) 27–43, https://doi.org/10.1016/j.ccr.2016.11.006.
[34] L. Abou Zeid, A. Pell, T. Tytus, P. Delangle, C. Bresson, Separation of multiphosphorylated cyclopeptides and their positional isomers by hydrophilic interaction liquid chromatography (HILIC) coupled to electrospray ionization mass spectrometry (ESI-MS), J. Chromatogr. B 1177 (2021) 122792, https://doi.org/10.1016/j.jchromb.2021.122792.
[35] M. Amaral Saraiva, P.E. Reiller, C. Marie, C. Bresson, Developing and downscaling a method by HILIC coupled simultaneously to ESIMS and ICPMS to determine the affinity of lanthanide chelating molecules using specific isotope dilution, J. Anal. At. Spectrom. 38 (2023) 2674–2690, https://doi.org/10.1039/D3JA00263B.
[36] L. Beuvier, C. Bresson, A. Nonell, L. Vio, N. Henry, V. Pichon, F. Chartier, Simple separation and characterization of lanthanide–polyaminocarboxylic acid complexes by HILIC ESI-MS, RSC Adv. 5 (2015) 92858–92868, https://doi.org/10.1039/C5RA16078B.
[37] N.M. Edelstein, J. Fuger, J.J. Katz, L.R. Morss, Summary and comparison of properties of the actinide and transactinide elements, L.R. Morss, N.M. Edelstein, J. Fuger (Eds.). The Chemistry of the Actinide and Transactinide Elements, Springer Netherlands, Dordrecht, 2006, pp. 1753–1835, https://doi.org/10.1007/1-4020-3598-5_15.
[38] F. Lahrouch, A.C. Chamayou, G. Creff, M. Duvail, C. Hennig, M.J. Lozano Rodriguez, C. Den Auwer, C. Di Giorgio, A combined spectroscopic/molecular dynamic study for investigating a methyl-carboxylated pei as a potential uranium decorporation agent, Inorg. Chem. 56 (2017) 1300–1308, https://doi.org/10.1021/acs.inorgchem.6b02408.
[39] J. Fèvre, E. Leveille, A. Jeanson, S. Santucci-Darmanin, V. Pierrefite-Carle, G. F. Carle, C. Den Auwer, C. Di Giorgio, Chelating polymers for targeted decontamination of actinides: application of PEI-MP to hydroxyapatite-Th(IV), IJMS 23 (2022) 4732, https://doi.org/10.3390/ijms23094732.
[40] F. Lahrouch, B. Siberchicot, J. Fèvre, L. Leost, J. Aupiais, P.L. Solari, C. Den Auwer, C. Di Giorgio, Carboxylate- and phosphonate-modified polyethylenimine: toward the design of actinide decorporation agents, Inorg. Chem. 59 (2020) 128–137, https://doi.org/10.1021/acs.inorgchem.9b02014.
[41] G. Creff, S. Safi, J. Roques, H. Michel, A. Jeanson, P.L. Solari, C. Basset, E. Simoni, C. Vidaud, C.D Auwer, Actinide(IV) deposits on bone: potential role of the osteopontin–thorium complex, Inorg. Chem. 55 (2016) 29–36, https://doi.org/10.1021/acs.inorgchem.5b02349.